Appl Phys B (2011) 105:67–79
DOI 10.1007/s00340-011-4764-0

**Applied Physics B**
**Lasers and Optics**

# Fluorescence spectroscopy of ultrathin molecular organic films on surfaces

**M. Müller · A. Langner · O. Krylova · E. Le Moal · M. Sokolowski**

Received: 27 May 2011 / Revised version: 21 July 2011 / Published online: 22 September 2011


**Abstract** We review our recent experiments by linear optical spectroscopy in the visible spectral range on interface controlled monolayers and thin films of $\pi$-conjugated organic molecules on well-defined surfaces. In particular, cw fluorescence and fluorescence excitation spectroscopy are considered. We discuss two interesting aspects: the possibility to prepare interface controlled films with non-bulk like structures, and consequently different and possibly superior optical properties, and the use of optical spectroscopy as an analytical tool to investigate properties of interfacial organic films.

## 1 Introduction

The optical properties of $\pi$-conjugated organic molecules in the condensed state have been a subject of major interest over the last years under both fundamental [1] and applied aspects [2]. The latter are in particular motivated from the development of organic light emitting devices (OLEDs) and organic photovoltaic cells (OPVCs) on the basis of thin semiconducting organic films prepared by vapour deposition onto solid substrates. Very important in this context is the strong correlation of resulting electronic and optical properties with structural and morphological properties in organic thin films. Since thin films can be structurally very different from the respective molecular bulk crystals, they can also exhibit different and novel optical properties. These may be decisive for their operation as a part of an active optical device, e.g., an OLED. This aspect has indeed motivated experiments on the optical properties of thin films with a range in thickness from several nanometers to a single monolayer of molecules or even to the limit of isolated molecules deposited onto a solid substrate surface. Obviously, the thinner the films are the more important becomes the interface to the substrate surface. Hence, meaningful experiments on very thin organic films require a control and a high definition of the substrate surface by the use of surface science methods.

An important aspect of optical excitation in condensed molecular systems is delocalization. The theoretical description of delocalized optical excitations in organic condensed matter, in particular in the crystalline state, is already rather well established and is based on the concept of Frenkel excitons. It was introduced by Davydov in the 1960s [3]. The Coulomb coupling of the excited molecular state on a molecule to other molecules in the solid, that is often described in the approximation of a dipole–dipole coupling of the respective transition dipoles, leads to delocalization of the excitation and formation of exciton bands [4]. The properties of these bands, for instance, the width of the band and the position of the energetic minimum in $k$-space, depend on the detailed structural arrangement of the molecules within the crystal [4, 5]. They are decisive for the resulting optical properties, e.g., the fluorescence yield. As a consequence, for organic molecular crystals, there exists a relationship between the structural and the optical properties. One of the first experiments which tested this relationship by a deliberate change of the structural arrangement was that of Kirstein et al. [6, 7]. The authors followed the variation in the absorption spectra of a Langmuir film that was compressed on the water surface in a trough.

Today, the optical experiments on organic molecules close to an interface to a substrate can be divided on the ba-

M. Müller · A. Langner · O. Krylova · E. Le Moal · M. Sokolowski (✉)
Institut für Physikalische und Theoretische Chemie der Universität Bonn, Wegelerstraße 12, 53115 Bonn, Germany
e-mail: sokolowski@pc.uni-bonn.de
Fax: +49-228-732551

sis of the thickness of the molecular films into three groups: (a) experiments on thin epitaxial films (with a thickness of several molecular layers), in particular, on such films which exhibit a structure different to that of the known bulk crystals of the respective molecules, (b) experiments on molecular monolayers which resemble true two-dimensional systems and hence have optical properties different to bulk crystals, and (c) experiments on isolated molecules on surfaces, for which the intermolecular coupling effects are negligible.

The aspects of interests in these experiments are numerous. Roughly speaking, one can identify two categories. The first comprises those experiments which investigate the implications of the substrate surface on the optical properties. Hereby, one aspect is to understand the interplay of the interface controlled structural arrangement and the resulting optical properties. Most appealing in this context is the use of the interface to the substrate surface to induce molecular structures which have optimal or special optical properties, e.g., a strong fluorescence due to a J-aggregate-like intermolecular coupling [8], resulting from a surface induced parallel arrangement of the molecular transition dipoles. In addition, molecular layers on surfaces allow very controlled investigations of the relation between the quality of their structural order, e.g., the size of ordered domains, and the resulting line widths in optical spectra. Another aspect of interest is charge transfer across the interface [9, 10] or rapid quenching of the fluorescence by the interface to the substrate surface [11]. This latter aspect is in particular relevant, when fluorescence spectroscopy of molecules directly bonded to the substrate surface is considered.

The second category contains experiments which use optical spectroscopy as an analytical method to study molecules on surfaces. This type of experiments aims at information on various aspects, e.g., the structures of molecular layers, phase transitions between different structural phases, and kinetic aspects of molecules, as for instance diffusion and aggregation into ordered domains. Evidently, the number of experiments in this category is presently still very small, since optical spectroscopy in the visible spectral range on molecules on surfaces is a rather novel field of research. In particular, experiments on well-defined surfaces, i.e., single crystal surfaces that are prepared and controlled by state of the art surface science analytic techniques and on which the molecules are adsorbed on chemically and structurally well defined sites, and hence lead to clear spectroscopic features are rare. The interpretations of earlier experiments which have been performed for instance on dyes deposited from solution on solid substrates, often suffer from the absence of a well-defined structural situation of the molecules on the surface [12–15].

In this review, we report on some sample systems which we have studied over the last years under the aim to establish optical spectroscopy as a tool to study molecules on well-defined single crystal surfaces. We have concentrated on fluorescence spectroscopy in the visible spectral range. This had the implication that for investigations on monolayers in direct contact to the substrate interface we had to find sample systems where fluorescence is present, and not quenched as it occurs on a metallic substrate. However, since we also wanted to use electron based surface science techniques, in particular low energy electron diffraction, for structural control, the samples had to allow for some charge conduction at the same time. The response to these two conflicting demands turned out to be difficult, as we will report below. We will discuss our results also in the context of important findings of other groups, although we will not be able to give a complete review of the field here.

## 2 Experimental aspects

### 2.1 Methods

Most easily photoluminescence (PL) or fluorescence (FL) spectroscopy can be performed on any samples as long as the signal is strong enough for detection (and is not hidden by a strong fluorescence of the substrate). Obviously, optical absorption spectroscopy can be only used as long as the substrate materials are transparent, as it is the case, e.g., for glass, mica [16], or potassium hydrogen phthalate (KAP) [17]. For nontransparent substrates, e.g., HOPG [18], $SiO_2$ [19], or metallic substrates [20], differential reflection spectroscopy (DRS) [19, 21], or spectral ellipsometry [22, 23] can be used instead, because these techniques also yield information on the imaginary part of the dielectric constant and hence on the absorption coefficient of the film. The large advantage of these latter techniques is that they do not require fluorescence of the molecules. This allows in particular the investigation of molecular films on metal surfaces, where the fluorescence of the first and often even the second layer is quenched below the detection limit [11]. The disadvantage is obviously that small film thicknesses lead only to small variations in the intensity of the reflected light. As a consequence, a very stable and reproducible positioning of the sample for the two required spectral scans (prior and after the film deposition) are required. This may limit a variation of the temperature of the sample, in particular the possibility to cool it. Another advantage of DRS is that data acquisition is fast and can be done in-situ during film growth. For further details of DRS, we refer to the review by Forker et al. [21]. Reflection absorption spectroscopy (RAS) [17], also named reflectance difference spectroscopy RDS [24], is similar to the above techniques. The advantage of this technique is that only a single spectral scan is required. However, it requires anisotropic substrate surfaces, e.g., $TiO_2$ [24], Cu(110) [25], or KAP(010) [17].

A third possibility to measure the absorption is the use of fluorescence excitation spectroscopy (FLE), also named more generally PLE (photoluminescence excitation spectroscopy). The large advantage of this technique is that again only a single spectral scan is required and that it is a background free method. This latter aspect leads to a very high signal to noise ratio that allows to measure smallest quantities of molecules, as it is done, e.g., in traditional single molecule spectroscopy experiments [26]. In addition, temperature variation of the sample does not constitute a problem for PLE. In particular, low sample temperatures which are attractive as the lines become generally much narrower can be accomplished. The disadvantage of this technique is that it requires fluorescence and is hence not applicable whenever rapid quenching occurs, e.g., for the first layers on a metal surface [27, 28]. In addition, the experimental setup is more sophisticated, since for thin films and high spectral resolution the excitation must be performed by a wavelength tunalbe laser. Often dye lasers are used for this purpose, which have only small and hence less favorable tuning ranges with respect to the absorption spectra of the molecular species.

In order to measure the fluorescence of very thin films [29], monolayers [30, 31], or isolated molecules [32, 33] on surfaces, one can alternatively use excitation of the molecule by the tunnelling current under the tip of a scanning tunnelling microscope. This technique, electroluminescence scanning tunnelling microscopy (EL-STM), has been explored by several groups over the last years. (For a recent review, see [34].) Concerning the quenching of the excitation by nonradiative decay process, the same limitations as for fluorescence spectroscopy apply. However, the electron induced excitation of the molecule may be different to that of a conventional optical far field excitation, and in the detection channel the STM tip plays an additional role due to coupling to a tip plasmon [35]. As a consequence, there presently exists an ongoing discussion on the interpretation of EL-STM spectra in relation to far field PL spectra. Nevertheless, this technique offers an interesting approach to optical properties of molecules on surfaces, since it allows recording the structural situation of the molecule in parallel with the optical properties. It can be hence expected that EL-STM will be valuable, e.g., when the intermolecular coupling of optical excitations in small well-defined clusters of molecules is studied.

For the experiments reported here, it was further mandatory to measure the structural order of the substrate surfaces and the prepared molecular films. We have in particular used low energy electron diffraction (LEED), which has the advantages that it can be easily performed at low temperatures and that it is a statistically averaging method as optical spectroscopy. Hence, structural information from LEED, e.g., the fraction of a specific structural phase, can be directly compared to information obtained by optical spectroscopy.

## 2.2 Sample systems

Typical $\pi$-conjugated molecules that are suitable for the preparation of organic thin films by vapour deposition exhibit a mass between 200 and 600 amu. Smaller molecules tend to have too high vapor pressures to form stable films under vacuum and to possess optical gaps that are too far in the UV spectral range. An attractive aspect is that vapor deposition permits to grow films with deliberately chosen nominal thicknesses from the sub-monolayer range up to films of many molecular layers. In the following, we give the film thicknesses in number of monolayers (ML), i.e., the molecular area density of the first completed monolayer of the respective molecule/substrate combination.

Figure 1 shows the structure formulas of three model molecules which we have studied on surfaces in our experiments, namely tetracene (Tc), rubrene (Rub), and perylene-3,4,9,10-tetracarboxylic acid dianhydride (PTCDA). Other examples of $\pi$-conjugated molecules which have been studied by optical spectroscopy as thin films are: oligothiophenes ($\alpha$-4T, $\alpha$-6T) [17, 36], pentacene (PEN) [37], quaterrylene [38], diindenoperylene (DIP) [37], phthalocyanines [23, 39], porphyrins [32], and *para*-sexiphenyl (p-6P) [24].

For Tc and Rub, the transition dipole moment of the relevant and allowed $S_0$–$S_1$ transition is oriented along the short axis, and hence *perpendicular* to the long molecular axis (along the *M* axis) [40]. On the contrary, it is oriented *along* the long axis for PTCDA [41]. Tc and PTCDA are both planar molecules. For Rub the four phenyl groups are rotated out of the molecular plane, and in addition the Tc backbone of Rub is twisted in solution or gas phase [42]. In Rub crystals, however, the backbone is planar again [43]. Due to the phenyl groups Rub forms an orthorhombic crystal structure [44] significantly different from the monoclinic crystal structure of Tc [45]. The Rub molecules are arranged on the *ab* planes whereby the short *M* axes of the molecules are all parallel to the *c* axis ("pin cushion" arrangement), and consequently the transition dipoles on the *ab* planes are all in a parallel orientation. If one neglects the intermolecular coupling along the *c* axis due to the larger spacing along this direction, this in plane coupling of parallel transition dipoles corresponds to that in linear H-aggregates [46]. As a consequence of the intermolecular dipole coupling, one expects a decrease of the exciton band towards the Brillouin zone edge. This is in contrast a head-to-tail coupling in a linear arrangement of the transition dipoles that is referred to as a J-aggregate and which leads to a minimum of the exciton band at the center of the Brillouin zone ($k = 0$) [8]. Due to the inductive effect of the phenyl substituents mainly on the highest molecular orbital, the $S_0$–$S_1$ transition of Rub is red-shifted with respect to that of Tc [42]. We note further that PTCDA exhibits a quadrupole moment with negative partial charges on the two terminating anhydride groups that is very

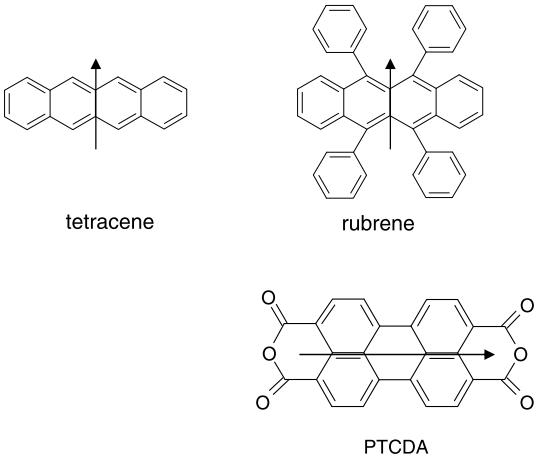


**Fig. 1** Structural formulas of fluorescent molecules considered in the text. The directions of the transition dipoles of the relevant optical transitions ($S_0$–$S_1$) are indicated by the arrows. Note that rubrene is not planar

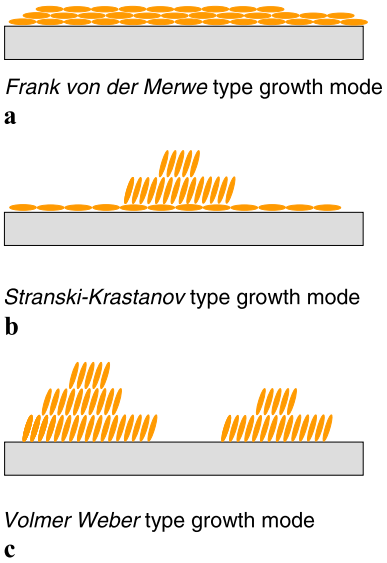


**Fig. 2** Schematic illustration of the three principle growth types (**a** to **c**) of thin films adapted for $\pi$-conjugated organic molecules at small coverages. The orientation of the conjugated $\pi$-system is indicated by the elongated shape of the molecules. Here, we have made the very plausible assumption that a stronger interfacial interaction with the substrate tends to orientate the $\pi$-system parallel to the surface. For further details, see text

relevant for the intermolecular interaction in the bulk and in layers on surfaces [47].

As mentioned already above, structurally defined sample systems can be achieved on well-defined surfaces only. Hence, the choice of the substrate surface is essential. In the past, in particular coinage metal surfaces (Au, Ag, and Cu) have been used very successfully as substrates for studying growth of $\pi$-conjugated molecules [48, 49]. Due to a moderate chemisorptive bonding of the molecules to these surfaces via their $\pi$-electron systems an ordered wetting layer with flat-lying molecules is formed (see Fig. 2(a) and (b)). If the corrugation of the surface potential is strong enough, the monolayers form superstructures that are commensurate in first or higher order with the substrate surface. Otherwise, ordered structures with a reduced lattice coincidence, as described by the point-on-line [50] or the line-on-line principle [51] form. From the second layer onward, the films grow epitaxially in the Frank-van der Merwe or Stranski–Krastanov growth type. As a consequence, in some cases, interesting nonbulk like structures can be stabilized by the interface to the substrate. In addition, for not too large band gaps, the charge conduction of the semiconducting molecular films is usually sufficient to allow their analysis by electron based techniques.

However, fluorescence quenching at the organic/metal interface discards metals as substrates for fluorescence experiments on adsorbed monolayers. For this purpose wide-gap (dielectric) materials have been used as substrates, either in the form of bulk crystals (NaCl [52], KCl [52, 53], potassium hydrogen phthalate (KAP) [17], sapphire [54]), or in the form of thin epitaxial films that were deposited on metal or semiconductor substrates [36]. The use of these epitaxial films is in particular attractive, since if these are thin enough, sufficient electron tunnelling into and out of the underlying conductive substrate is possible and allows using electron based techniques for further spectroscopic or structural investigations. In our investigations, we have used thin aluminium oxide ($AlO_x$) films that can be grown epitaxially in a self-terminating fashion on the $Ni_3Al(111)$ surface by annealing the sample in an oxygen atmosphere [55], or thin films of NaCl [56–58] and KCl [59] that were obtained by deposition of the respective salts from thermal evaporation sources onto the Ag(100) surface. In both latter cases, films of varying thickness with large flat surface terraces could be obtained. We note that this approach of using thin epitaxial dielectric films is also used successfully for the decoupling of small catalytic nanoparticles [60] and molecules that are subject to detailed STM investigations [61].

Due to their small chemical reactivity, the bonding of molecules to surfaces of dielectric materials is weaker compared to that on metal surfaces. For pure hydrocarbons, as Tc and Rub, it is based mainly on van-der-Waals forces. As a consequence, intermolecular forces between the extended $\pi$-orbitals are often stronger than those between the $\pi$-orbitals and the substrate surface and cause that molecules tend to pack in an up-on-edge orientation with respect to the substrate surface on dielectric materials, as illustrated in Fig. 2(c). For molecules which exhibit partial charges on their functional groups (e.g., PTCDA), additional Coulomb forces between these and ions of the substrate surface may play a role and favor a flat-lying orientation. However, due to the generally smaller interfacial bonding on dielectric surfaces, the tendency of adsorbed molecules to dewet from the

interface and to aggregate in three-dimensional clusters with bulk-like crystals structures is more pronounced on dielectric compared to metal substrates [62]. As a consequence, a Volmer Weber type growth (see Fig. 2(c)) is rather likely. Concerning surface experiments, this growth scenario is of course less desired, since the interface to the substrate is of minor importance then, and since the clusters usually cover only a small surface fraction which makes them "invisible" for averaging surface science techniques, as for instance LEED. For optical experiments the formation of a complete wetting layer on a dielectric substrate is hence the favored situation.

## 3 Optical spectra of thin films

### 3.1 The role of the structural packing

We start by reporting experiments which were performed on thin films of Tc. In combination with this molecule, we utilized two substrates, namely $AlO_x/Ni_3Al(111)$ [54] and Ag(111) [63]. For the time being, we only discuss the luminescence of thin films and the role of structural packing for it. Quenching effects at the substrate interface will be considered below.

Figure 3 displays PL spectra that were measured on the $AlO_x$ surface. At present, the spectra (a) and (b) are relevant; the spectra (c) and (d) will be discussed in Sect. 4.1 below. In general, the spectra (a) and (b) correspond to the spectra which are observed for free standing bulk Tc crystals at low temperatures (see refs. given in [64]). The emission at 18 600 $cm^{-1}$ is related to the 0–0 transition of a free exciton (marked F′ in Fig. 3); while the three broad peaks (marked as 1 to 3 in Fig. 3) on the low energy side of F′ are due to non-intrinsic decay channels related to a self trapped exciton (1) and radiative traps (2, 3) [64]. The noted agreement of the spectra with those of bulk crystals indicates that the structural arrangement of Tc in the film on $AlO_x$ and in bulk crystals is identical or at least very similar. This conclusion is also corroborated by LEED experiments on these films which show that the Tc molecules have arranged in layers on $AlO_x$ that have a structure very close to that of the *ab* plane of Tc bulk crystals. The long axes of the molecules are nearly upright with respect to the $AlO_x$ interface, as it is illustrated in the inset in Fig. 3. There are two Tc molecules per unit cell, and the transition dipoles (along the short molecular axes) form a herringbone (HB) pattern that is parallel to the interface. However, due to the rather weak interaction at the interface, Tc domains or crystallites on $AlO_x$ are azimuthally disordered, which leads to diffraction rings in the LEED pattern [54].

A comparable PL spectrum can be also obtained, when a Tc film is grown on the Ag(111) surface. However, here the

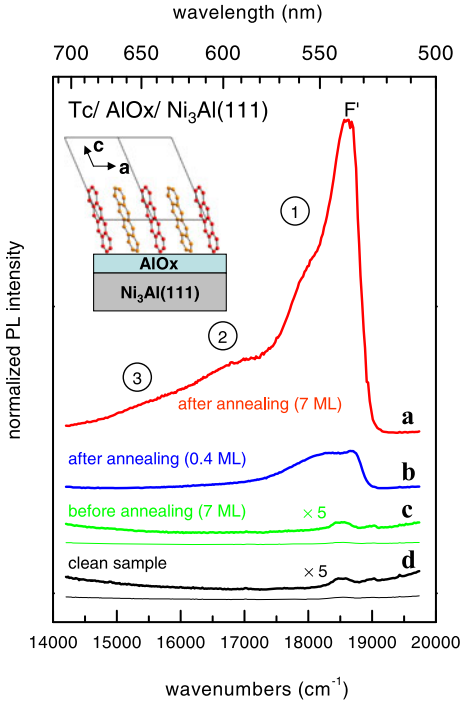


**Fig. 3** (Color online) Photoluminescence spectra of a *thin* Tc films on the alumina surface. (**d**) spectrum of the clean alumina surface for comparison. (**c**) after deposition of nominally 7 ML of flat lying Tc molecules at 45 K. (**b**) and (**a**) spectra of Tc films with a nominal thicknesses of 0.4 ML and 7 ML after an additional slow warming cycle up to 240 K with about 10 K $min^{-1}$. All spectra were measured at 45 K. The excitation wavelength was 458 nm (21 800 $cm^{-1}$, 2.702 eV). The small peak at about 18 500 $cm^{-1}$ in the magnified spectra (d) and (c) is an artifact, likely from the glass window of the UHV chamber. The very small peak at 19 500 $cm^{-1}$ is a plasma line from the Ar laser. The spectra are vertically shifted against each other for clarity. The inset illustrates the structural model for Tc in the ordered film. Further details see text. Reproduced from [63]

orientation of the long molecular axes is parallel to the interface and the above noted herringbone pattern of the transition dipoles is thus perpendicular to the surface. This is illustrated in Fig. 4(a). As described in detail by Lim et al. [65, 66], a consequence of this structural arrangement and the related coupling of the transition dipoles is the formation of an exciton band structure with an energetic minimum at $k = 0$ (similar to the situation in a J-aggregate), leading to a weak superradiance in Tc crystals [65] and films [64] at low temperatures.

Notably, Tc films with prominently different PL spectra can also be obtained on Ag(111) (see Fig. 5). These "narrow" spectra show a significant reduction of the line width by a factor of about 3 with respect to those "broad" spectra of Tc films considered so far, in particular when the sample is cooled to low temperatures. In addition, the pure electronic transition is strongly enhanced and the vibronic side bands are suppressed. For $T \approx 50$ K, we obtain a $FWHM_{0-0}$ of $\sim$175 $cm^{-1}$ and $\sim$150 $cm^{-1}$ in the PLE and PL spectra, respectively. Unfortunately, the structural arrangement

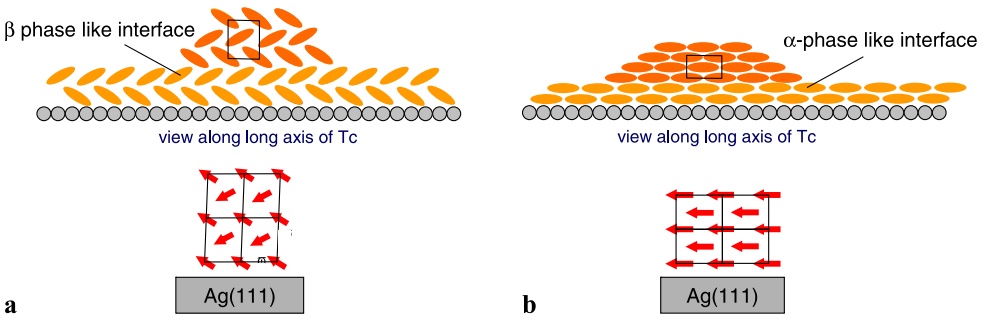


**Fig. 4** Schematic illustration of the growth of Tc films on the Ag(111) surface in two different polymorphic structures. The resulting arrangement of the transition dipoles is shown below the respective structures. For further details, see text

of the molecules in the crystallites on the wetting layer could not be clarified directly, since a pronounced Stranski–Krastanov growth occurs, making the footprints of the crystallites too small to yield significant diffraction signals in LEED. However, from the phase diagram of the first monolayer of Tc on Ag(111) [63] and the optical spectra themselves, there is good evidence that in contrast to the films considered so far, the molecular planes in these latter films are all parallel to the interfaces, as illustrated in Fig. 4(b). Hence, the structural arrangement is considerably different to that of Tc bulk crystals, and we suggest that the transition dipoles are arranged in the illustrated brick wall (BW)-like structure (Fig. 4(b)).

From the phase diagram of Tc adsorption on the Ag(111) surface, the growth of these two different polymorphic structures of Tc can be understood as following. For coverages up to one monolayer (ML) Tc forms the so-called well ordered $\alpha$ phase on Ag(111), where all molecules are planar on the surface [63]. For the film growth that proceeds on this $\alpha$ phase, it is feasible that the fully parallel orientation of the molecular planes is maintained. Hereby, the first interfacial layer acts as a template for the orientation of the molecular planes of the higher layers. In contrast to that, at higher monolayer coverages from about 1.3 ML onward, Tc forms a second more compressed $\beta$ phase on Ag(111), where the molecules are partly non-planar and tilted out of the plane of the interface [63, 67]. Further film growth on this $\beta$ phase presumably proceeds in a bulk-like phase with a nonuniform orientation of the molecular planes, leading to a HB-like arrangement of the transition dipoles as illustrated in Fig. 4(a). As described in [63], the sample temperature during growth decides, whether the multilayer layer growth proceeds on the $\alpha$ phase or the $\beta$ phase.

How can one understand these two different types of PL spectra on the basis of the structural data? Of course a higher density of structural defects in those films yielding "broad" spectra with respect to those yielding "narrow" spectra is feasible on the background of the above different growth scenarios. Generally, structural defects lead to line broadening by inhomogenous line broadening and radiative traps. In addition, the different structures can also have a profound, intrinsic effect on the spectra. In all examples considered by us, we have found that the effect of the structural order on the optical spectra can be intuitively understood from the interaction of the transition dipoles. This approach is based on a weak coupling of the excited states and calculates the exciton energies from a perturbative solution (for details, see, e.g., [4]). Concerning the HB and BW arrangement of the transition dipoles in the structures of Tc on Ag(111) this predicts a more attractive interaction of the dipoles in the linear arrangement in the BW structure compared to that in the HB structure [6, 7, 68]. In particular, it is known that a BW structure leads to a pronounced attractive coupling and J-aggregate-like emission in molecular solids, whereas the coupling in the HB structure, also being still attractive, is considerably weaker. As a consequence superradiant emission occurs from the BW structure of Tc on Ag(111), leading to an increased emission rate $k_{\mathrm{rad}}$ and a dominance of the 0–0 transition with concomitant suppression of the vibronic side bands. We expect to see this increase of $k_{\mathrm{rad}}$ most pronounced in time resolved PL experiments for the BW structure, similar as it has been for Tc films on HOPG [64] or quaterthiophene (4T) films on KAP by Meinardi et al. [69], but which are today not available yet.

Most prominent is of course the strong line narrowing in the PL spectrum of the BW phase when going from 200 to 48 K (see Fig. 5). We explain this by a *motional line narrowing* effect [70], as it was introduced for strongly coupled J-aggregates by Knapp [71]. The physics behind this is that at lower temperatures the exciton wave function becomes more and more delocalized, and hence averages over the static inhomogeneous energetic disorder in the film that is caused by structural defects, and which usually determines the line width in emission. As a consequence of the motional narrowing, the PL line width is reduced at low temperatures. The effect is the more pronounced the larger the number of molecules $N_C$ is which coherently contribute to the exciton. In a simple picture, $N_C$ is the larger the stronger the intermolecular dipole coupling is [72, 73]. This makes it understandable that the effect is relevant for the BW structure of Tc on Ag(111), whereas it is about nonobservable for the HB structure of Tc on Ag(111).

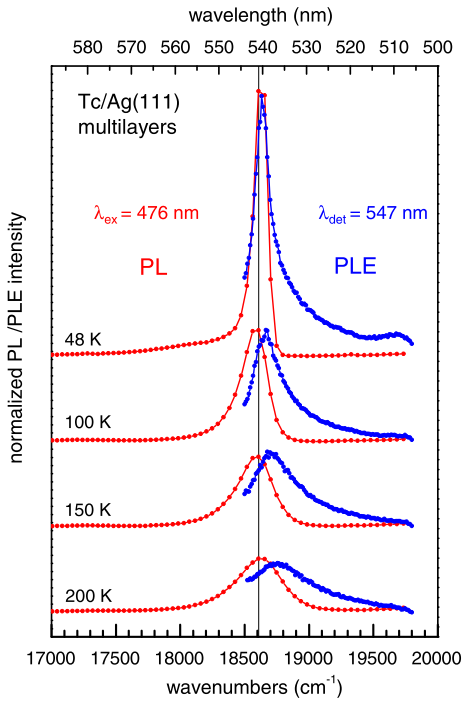


**Fig. 5** (Color online) Photoluminescence (PL, *red*) spectra and PL excitation (PLE, *blue*) spectra of a *thin* Tc film on the Ag(111) surface as a function of temperature. Both sets of spectra were normalized at their respective maxima at 48 K. The nominal film thickness was about 6 monolayers. For further details, see text. Taken from [89]

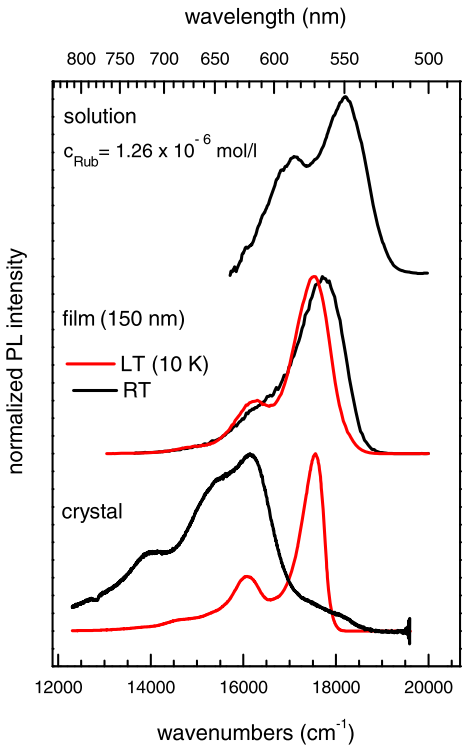


**Fig. 6** (Color online) Overview on PL spectra of Rub. *Top*: dissolved in cyclohexane (details see [42]), *middle*: in the form of an amorphous film on glass, and *bottom*: for a single crystal. The two lower pairs of spectra were measured at room temperature (RT) and at about 10 K. Taken from [90]

### 3.2 Intermolecular screening

Rub has the interesting property that thin films prepared by vacuum sublimation are amorphous [43, 74]. As discussed by Käfer et al. [43], the effect is explained as a consequence of an activation barrier that has to be overcome when the twisted molecules transit into the planar configuration upon formation of the crystal. Figure 6 gives an overview on PL spectra of Rub in solution, in the form of a thin film, and as a crystal. For the two latter samples, the spectra were recorded at room and at low temperatures. In the following discussion, we consider the crystal spectrum at low temperature, since at higher temperature the emission presumably occurs from significantly red-shifted states, e.g., luminescent traps, and is hence not intrinsic [75]. All three spectra in Fig. 6 show a clear (unresolved) vibronic replica at an effective energy of 1500 $cm^{-1}$ with respect to the main peak related to the 0–0 transition.

As expected, Rub films deposited on $AlO_x$ are amorphous, too. This was concluded from the observation that no new diffraction features appeared in the LEED images upon deposition of Rub. For a deposition at low temperatures, as it is discussed in the following, the surface is homogenously covered, as concluded from the fading of the $AlO_x$ LEED spots

Figure 7 displays a series of Rub PL spectra taken for films of increasing thickness which were deposited at low temperatures. Two results are interesting here. First, the photoluminescence yield decreases by about three orders of magnitude when the film thickness decreases from 100 Å to 0.6 Å (see also Fig. 8(b), below). The strong increase of the PL yield, with film thickness, is presumably due to the suppression of the energy transfer ("quenching") to the image dipole in the $Ni_3Al$ metal substrate for the larger film thicknesses, and consequently larger average molecule to substrate distances [76]. Nevertheless, the smallest nominal film thickness for which we could obtain a PL spectrum of Rub was 0.60 Å and must correspond to a coverage that is below that of a monolayer. (Using a nominal layer thickness of 3.7 Å, this would yield a coverage of about 15%.) As we will discuss in detail below, the data hence indicate that Rub molecules in direct contact to the $AlO_x$ interface are luminescent.

Secondly, Fig. 7 reveals that the PL spectra shift systematically to lower energies (by about 1200 $cm^{-1}$) with increasing film thickness. Two vertical lines, marked by A and B, indicate the positions of the 0–0 transition, that are measured for a thick Rub film (150 nm) at low temperatures and for Rub in solution (from Fig. 6), respectively. The spectra of thick films are consistent with those, obtained for

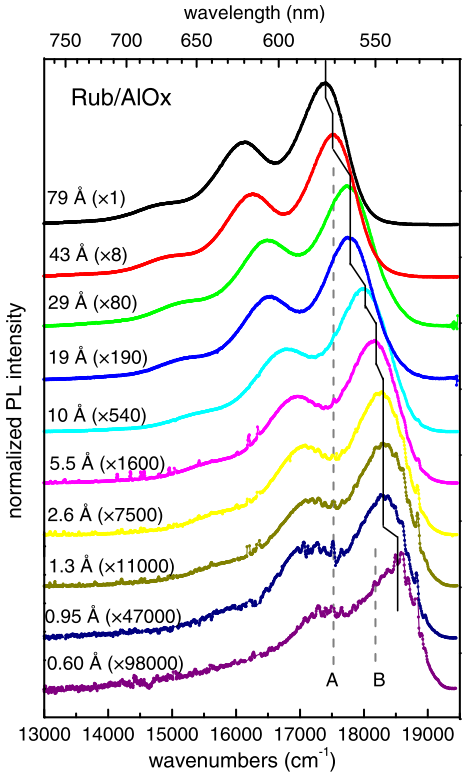


**Fig. 7** (Color online) Normalized PL spectra of ultrathin rubrene films on the $AlO_x/Ni_3Al(111)$-substrate for different nominal film thicknesses illustrating the systematic shift of the emission in energy with film thickness. The normalization factors for the PL are denoted in the figure. Note that the absolute PL intensity varies nearly by five orders of magnitude from the thinnest to the thickest films. Deposition of the molecules and the photoluminescence measurements were both performed at a substrate temperature of 40 K. The excitation wavelength was 496 nm. The solid vertical is a guide line for the eye to indicate the shifting of the 0–0 transition. The *dashed* two vertical *lines* A and B mark the positions of the 0–0 transition of the 150 nm thick Rub film on glass at low temperature and for Rub in solution in Fig. 6. Taken from [91]

thicker films deposited at room temperature (RT) on glass and cooled to 40 K afterward (see Fig. 6). Hence, large morphological and structural changes due to different deposition temperatures used in the two experiments, film thickness or different substrates can be also excluded. This convergence of the PL spectrum to that measured for a thicker amorphous film on glass gives additional support for the amorphous morphology of Rub on $AlO_x$. A further argument for the amorphous morphology is the rather large line width in the PL spectra.

The film-thickness dependent shift of the emission is interesting. In general, the intermolecular interaction on the optical transition yields has two contributions: a polarization screening of the excitation (often named as $D$ term [3]) and the dipole–dipole coupling related to the transfer of the excitation within the ordered lattice. Due to the amorphous morphology, the second contribution must be less effective here. Hence, the observed red-shift by up to 1200 $cm^{-1}$ with film thickness monitors the increasing polarization screening by surrounding Rub molecules with increasing thickness. Remarkably, for very small coverages on $AlO_x$, the 0–0 transition is shifted to higher energies with respect to that in solution (line B in Fig. 7). This possibly indicates that isolated Rub molecules are present on the surface at these low coverages, which are not subject to screening, either by solution molecules or other Rub molecules, on the vacuum side of the interface.

## 4 Optical spectroscopy of monolayers

### 4.1 Quenching of the luminescence

The most interesting but also, as it turned out, most challenging aim is to observe the luminescence from a monolayer with well-defined structural order. On metal surfaces, well ordered monolayers form, but the luminescence is quenched. For instance, we observed for PTCDA and quaterthiophene on Ag(111) that the onset of a measurable luminescence occurs upon deposition of the third layer [27]. An analogous situation was also found for Tc on Ag(111) (see Fig. 8(a)). The onset is related to the start of growth in the third layer on top of a "bilayer" of the $\beta$ phase. We note here that the original structure model of the $\beta$ phase of Tc on Ag(111) given in [63], was amended in the meantime by additional information from STM which showed that the $\beta$ phase is indeed a more complex two-layer structure and can take up a nominal coverage of 2.5 ML (1 ML corresponding to the coverage of the completed monolayer of the $\alpha$ phase) [67]. On the Ag(111) surface, a spacer layer of Tc molecules with a thickness of about 10 Å forming the $\beta$ phase (corresponding to about 2.5 layers of planar aromatic molecules) is hence necessary for luminescence.

On $AlO_x$ the luminescence appears to be related to the molecular orientation. PTCDA, which presumably adsorbs in a planar orientation, did not show any luminescence. We note that this was observed for PTCDA monolayer films where quenching effects due to aggregate formation are not expected. We did also not see luminescence of Tc films, directly after deposition at low temperatures (see Fig. 3, spectra (c) and (d)) [54]. This was true both for thin (submonolayer thick) films and thicker films. It was concluded that for the Tc thicker films grown at low temperature the disorder may play a role in addition to the interfacial effects and suppresses the luminescence below the detection level [54, 77]. Only after annealing the Tc films and inducing an upright orientation of the molecules (see Sect. 3.1 above), luminescence of the Tc monolayer could be detected. Only for Rub, a PL above the detection level was measurable on $AlO_x$ *directly* after the deposition (see Fig. 8(b)). We explain these

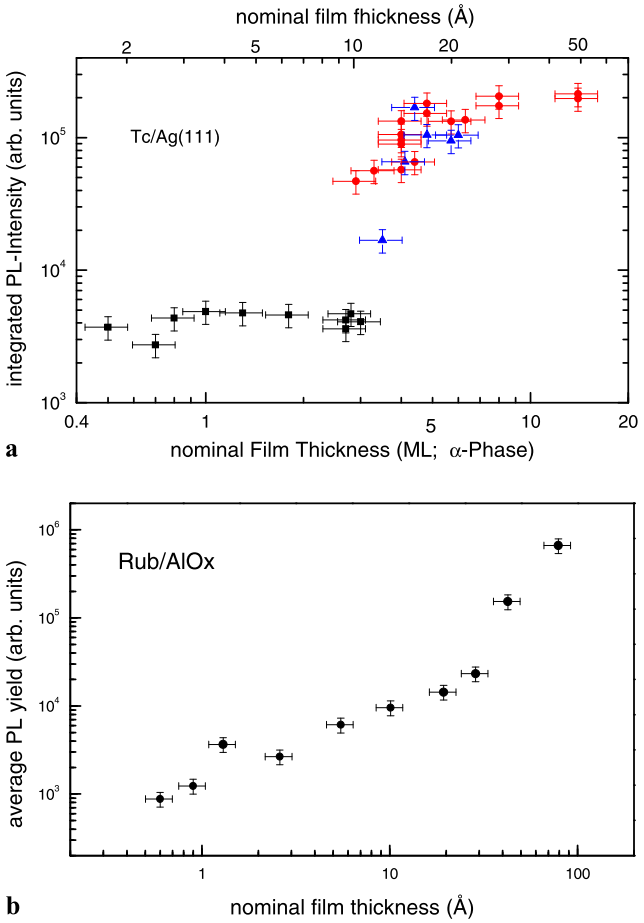


**Fig. 8** (Color online) (**a**) Spectrally integrated photoluminescence intensity of thin tetracene films on Ag(111) versus the nominal film thickness measure in monolayer (ML) of the $\alpha$ phase (*bottom axis*) and in Å under the assumption of a nominal thickness of 1 ML of 3.5 Å (*top axis*) [89]. The circles (*red*) refer to spectra similar to those in Fig. 3, the triangles (*blue*) to the narrower spectra of Fig. 5. The squares (*black*) indicate the level of background intensity. (**b**) Photoluminescence yield of thin rubrene films on $AlO_x/Ni_3Al$ versus the nominal film thickness [91]

findings by tunnelling of metal substrate states through the thin $AlO_x$ film into the molecular $\pi$ orbitals that are oriented in the plane of the surface [54]. This quenching mechanism can be obviously suppressed by a reduced overlap with the $\pi$ orbitals that can be achieved by either the noted upright position of the Tc, or the additional phenyl groups acting as spacer legs on Rub. Our result is in principle in agreement with the observation of luminescence under the STM tip (EL-STM) for Zn(II)-etioporphyrin on $AlO_x$NiAl(110) by Ho and coworkers [32], because this molecule possesses also additional side groups that function as spacer legs, similar to Rub. However, Ho and coworkers [33] observed also luminescence for the smaller Mg porphyrin on NiAl(110), in contrast to what we would have expected. Unfortunately, the structural situation of the Rub on $AlO_x$ was unsatisfactory, since no structural order could be observed by LEED.

For this reason we started to investigate PTCDA monolayers on thin epitaxial films of NaCl [78] and KCl [59] on Ag(100). We have performed these experiments mainly on NaCl and KCl films with a thickness of about 10 layers. This thickness still allowed LEED experiments but at the same time suppressed the luminescence quenching by the metal substrate, due to overlap of molecular with metal wave functions and radiative damping by interaction with the image dipole in the substrate [76]. Before we turn to the optical properties of PTCDA monolayers on these substrates, we briefly resume some of the structural details of these PTCDA monolayers.

### 4.2 Interfacial order on alkali halogenides

On both surfaces, NaCl(100) and KCl(100), long-range ordered monolayers of PTCDA can be obtained. For NaCl(100) this was first reported by Burke et al. [79] on the basis of AFM results. For KCl(100), Dienel et al. reported the first highly resolved AFM images of PTCDA [53]. Earlier investigations by Schlettwein et al. [52] on PTCDA/KCl(100) already indicated the growth of a PTCDA wetting layer on KCl(100), however, the authors could not clarify the structural arrangement. The same PTCDA structures are also found on the respective epitaxial NaCl/KCl films on Ag(100). On KCl(100), this is a commensurate brickwall structure (BW) [59], on NaCl, a commensurate quadratic (Q) structure is found [78]. The two structures are illustrated in Figs. 9(b) and 10(a). The commensurability with the underlying substrate is remarkable and is presumably related to the Coulomb interactions between the surface cations and the negatively charged anhydride groups, in particular the carboxylic O atoms on the four corners of the PTCDA molecule [53, 79]. It should be, however, noted that no firm experimental validation of the exact adsorption site of the PTCDA on these surfaces has been obtained yet.

As can be seen from the sharpness of the spots in the LEED pattern in Fig. 9(a), the structural order of PTCDA/KCl(100) is very good yielding domains of at least 100 Å in diameter [59]. In addition, to the known Q structure on NaCl, we could prepare a second ordered monolayer structure with a higher density and a herringbone arrangement of the molecules (HB*) on NaCl, which is very close to that of PTCDA layers in the respective bulk crystals (see Fig. 10(b)). We termed this phase by HB* in order to indicate its metastability and its small structural deviation from the HB unit cell of the PTCDA multilayers on NaCl [78]. In contrast to the Q structure (see Fig. 10(a)), the HB* structure is metastable and can be obtained in a limited temperature window only. It transits into the stable Q structure when the sample temperature is raised to 200 K. This phase transition can be followed by LEED scans taken after stepwise annealing as illustrated in the inset in Fig. 12 (below). From

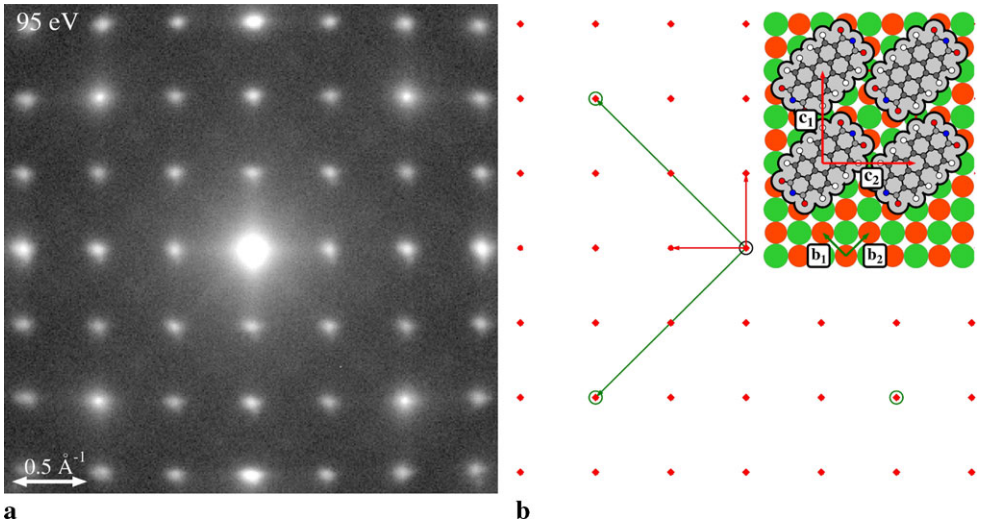


**Fig. 9** (Color online) (**a**) LEED pattern of 1 ML PTCDA adsorbed on 10 ML KCl on Ag(100) measured at an electron energy of 95 eV. (**b**) Simulated LEED and real space model of the brickwall structure of PTCDA on KCl(100). Reproduced from [59]

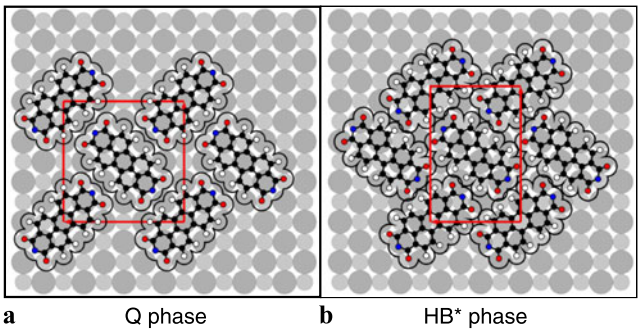


**Fig. 10** (Color online) Models of the two monolayer phases of PTCDA on NaCl(100): (**a**) the commensurate quadratic (Q) structure (unit cell: $16.92 \times 16.92$ Å$^2$), (**b**) the incommensurate rectangular herringbone (HB*) structure (unit cell: $13.5 \times 20.2$ Å$^2$). Reproduced from [80]

the relative fraction of the LEED intensities, the fractions of the two phases can be concluded and directly related with optical spectra recorded in parallel (see below) [80].

Utilizing NaCl and KCl films on Ag(100), it is hence possible to prepare three different monolayer structures of PTCDA (BW, Q, and HB*). These three structures resemble also the three canonic structures that are found, when PTCDA is adsorbed on the Ag(110), Ag(100), and Ag(111) surfaces, although the lattice parameters of the unit cells differ and the interactions between the PTCDA and the Ag substrate are different to those on the alkali halide surfaces [81–83].

### 4.3 Luminescence spectra and surface phase transitions

The luminescence of PTCDA adsorbed on NaCl and KCl is very strong and there is no difficulty to record PL spectra with good statistics for coverages in the range of a percent of a monolayer. In the following, we report spectra that were measured on NaCl. Those taken on KCl are of very comparable quality, but the effect of the intermolecular coupling on the spectra is of different strength due to the different structural arrangement of the molecules leading to a shift of the 0–0 position [84]. Figure 11 (middle) shows PL and PLE spectra that were taken after about 1% of a monolayer had been deposited at low temperatures (20 K) on NaCl. At these temperatures, the molecules are immobile on the surface, and statistically distributed isolated molecules are present. The respective spectra are well resolved, exhibit a dominant 0–0 transition, and show clear vibronic fine structure, in good agreement with that calculated for the free PTCDA molecule [85]. The Stokes shift, i.e., the energy difference measured between the 0–0 line positions in absorption and emission is very small ($<50$ cm$^{-1}$). The spectra differ considerably from those of PTCDA multilayers which are dominated by strong interlayer coupling of the stacked molecules and which are red-shifted by about 2000 cm$^{-1}$ [86]. This fundamental difference was seen first in PL spectra by Schlettwein et al. [52] and by DRS by Proehl et al. [16].

Condensation of the molecules into the ordered HB* or Q phase islands upon annealing of the sample can be observed in the optical spectra by a shift of the transition to lower energies. As discussed in detail in [80], the size of the shift can be understood as an effect of the intermolecular screening (polarization) and the exciton band structure formation. The size of the shift is specific for the respective structures (see inset in Fig. 11), and as explained in [80], can be quantitatively understood from the difference of the structures (Q vs. HB* on NaCl) leading to different intermolecular coupling of the transition dipoles and different intermolecular screening. From a comparison with the shifts on the basis of the calculated excitons bands, we estimate that the screening effect is of the order of 200 to 300 cm$^{-1}$. It is hence considerably smaller compared to that noted above

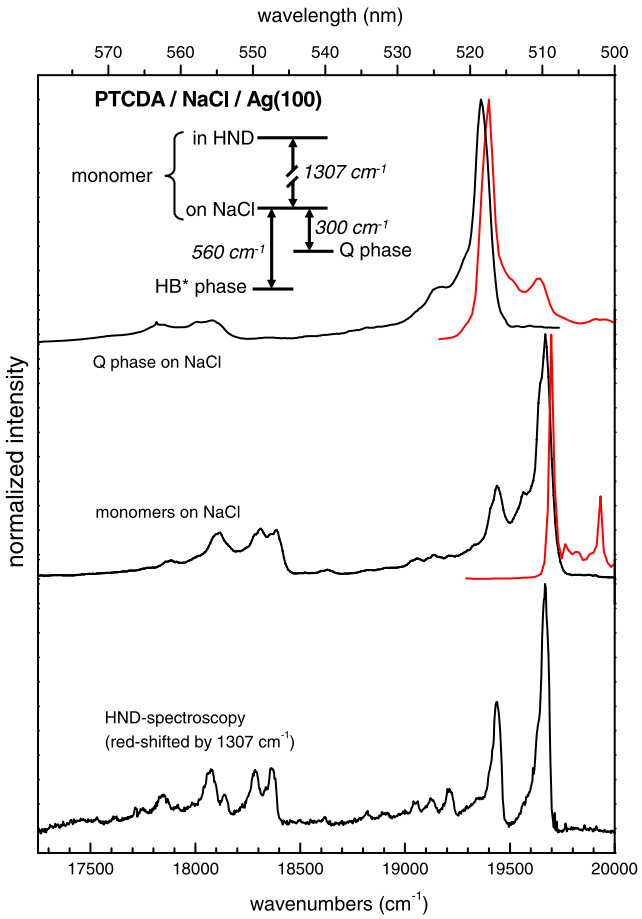


**Fig. 11** (Color online) Photoluminescence (PL, *left/black*) and PL excitation spectra (PLE, *right/red*) of the Q phase (*top*) and the diluted monomer phase (*middle*), both measured at a cryostat temperature of 20 K. The excitation wavelengths were 498 nm and 457 nm, respectively, whereas the detection wavelengths for the PLE spectra were 556 and 543 nm, respectively. In addition the PL spectrum of single PTCDA molecules in Helium nanodroplets (HND) (*bottom*) [88] is shown for comparison. This spectrum was red-shifted by 1307 $cm^{-1}$ in order to match the positions of the 0–0 transitions with those of the monomer spectra. The inset summarizes all relevant energy differences of the discussed phases. Reproduced from [80]

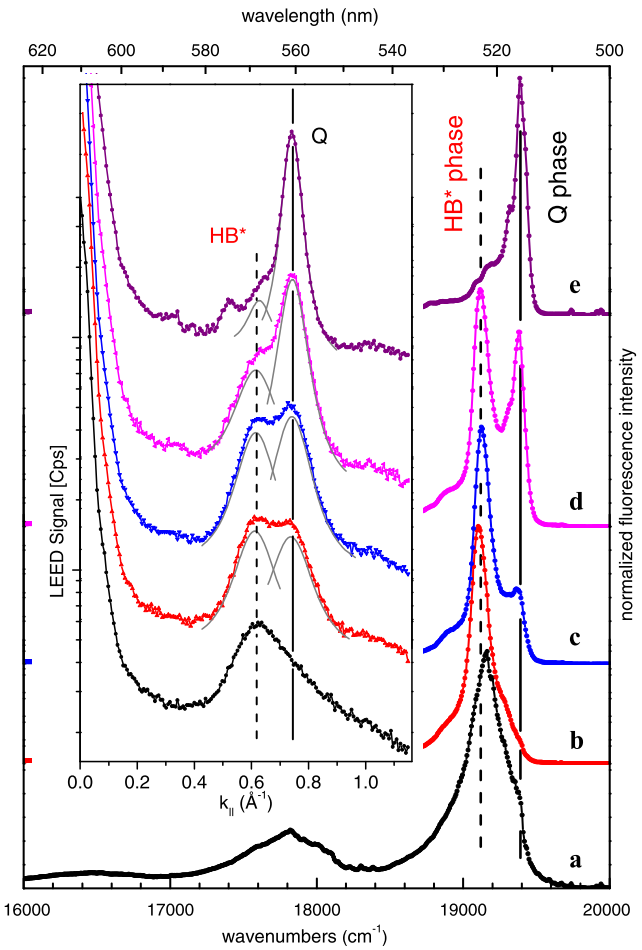


**Fig. 12** Fluorescence spectra (*right*) and LEED scans (*left*) obtained during the transition from the metastable HB* phase to the Q phase of PTCDA on NaCl(100). From (**a**) to (**e**), the fraction of the HB* phase decreases at the expense of the Q phase. This can be seen from the corresponding LEED scans on the left where the contributions of the HB* and the Q phase are indicated. For details of the LEED measurements, see [78]. The film thickness was 0.7 ML and deposited at 100 K. The transition was introduced by a stepwise and repeated annealing of the sample for 10 min at 200 K (**a**), +5 min 270 K (**b**), +10 min at 270 K (**c**), +10 min at 270 K and 10 min at 285 K (d), +30 min at 275 K and 20 min at 300 K (**e**). Reproduced from [80]

for Rub films (∼1200 $cm^{-1}$), which is nevertheless understandable from the 2D character of the PTCDA monolayer.

As illustrated in Fig. 11, the vibronic resolution of the PTCDA spectra on NaCl is nearly as good as that of the PL spectrum for PTCDA dissolved in ultra-cold He nanodroplets [87, 88]. The energetic positions of the vibronic sidebands are unaltered. Concerning the phase of isolated molecules this implies that (i) the NaCl surface does not have a major influence on the molecular vibrations and (ii) that the adsorption sites of the molecules must be rather well defined, since otherwise inhomogeneous line broadening would be expected due to a different polarization screening by the NaCl at the different sites. For the condensed Q phase, the same arguments hold true. However, concerning the line width, motional line narrowing related to the delocalization of the excitation plays an important role here, too [70]. We also note that the relative height of the vibronic sidebands with respect to the 0–0 transition is smaller for the Q phase in comparison to that of the phase of isolated molecules. This is a consequence of the coupling between the molecules, leading to a superradiant emission from the 0-0 transition and a suppressed coupling to the vibronic modes. Hence, we find an analogous situation in the PTCDA monolayer to that for thin Tc films with parallel orientation of the transition dipoles on Ag(111), described above.

Finally, we comment on the observation of the HB* to Q structure phase transition in the PL spectra that is illustrated in Fig. 12. In principle, the PL and the LEED spectra are superpositions of the two spectra belonging to the HB*

and the Q phase. During the phase transition, the intensity of the Q phase grows on the expense of that of the HB* phase. Both phases obviously exist in parallel on the surface during the phase transition. Notably, the intensity of the HB* phase in the PL spectra is stronger than its contribution in the LEED spectra would suggest (see, e.g., spectrum (d) in Fig. 12). This may be due to different quantum yields of the two phases and different relative intensities of the corresponding LEED spots. A direct consequence of this experiment is that any disorder in the monolayer will result in inhomogenous line broadening in the PL spectra of the order of the energetic shift between the 0–0 positions of the Q and HB* phases.

## 5 General conclusions and outlook

The examples discussed above illustrate that isolated organic molecules, condensed ordered monolayers, and thin films on surfaces can be investigated by fluorescence spectroscopy in the visible spectral range. The PL and PLE spectra give access to a rich variety of fundamental optical processes in condensed molecular solids. From the spectra one further derives information on the structural arrangement of the molecules, the energy transfer between different phases, and the presence of structural defects, e.g., domain boundaries, that lead to broadening of the spectra. Most interesting is obviously the concomitant direct access to and control of structural parameters, which is usually difficult for other sample systems that are subject to optical investigations. In principle, it is possible to follow kinetic processes, for instance the nucleation of deposited molecules into islands on the surface, from the evolution in the optical spectra in-situ and in real time. However, as reported, all these experiments require specific adsorbate systems, since otherwise structurally not defined film growth, clustering, and/or luminescence quenching may occur.

Most important for the interpretation of the spectra is the unambiguous determination of the structural arrangement. Concerning small (submonolayer) coverages further experiments performed by EL-STM would be interesting under this aspect. In particular, coupling of excitations in small molecular ensembles consisting of two to few molecules, could be studied by this technique. In our opinion, experiments which study coupling between different molecules in defined structural arrangement to each other would be attractive. Besides that one may consider to perform single molecule experiments on surfaces. From the experimental point of view, this would possibly require to go to even lower temperatures than those used here (20 K) to obtain smaller line widths. Besides the spectral isolation of the molecules in the frequency domain that is traditionally used for single molecule spectroscopy, an isolation in space by use of ultralow coverages in combination with light microscopy might be helpful for these experiments. From these experiments, it may be possible to find out interesting details of the diffusive motion of large organic molecules on the surfaces. Finally, a large range of time resolved optical experiments can be envisaged, also.

**Acknowledgements** We thank F. Stienkemeier for helpful discussion and making unpublished results available to us. We are further grateful to R. Scholz for advice on the theory of excitons. J. Pflaum has provided us with high quality rubrene crystals. The project was supported by the DFG Research Unit 557 and an Alexander von Humboldt fellowship (ELM).

## References

1. E.A. Silinsh, V. Čápek, *Organic Molecular Crystals* (Am. Inst. Phys., New York, 1994)
2. H. Klauk (ed.), *Organic Electronics* (Wiley, Weinheim, 2006)
3. A.S. Davydov, *Theory of Molecular Excitons* (Plenum, New York, 1971)
4. D.P. Craig, S.H. Walmsley, *Excitons in Molecular Crystals* (Benjamin, New York, 1968)
5. V.L. Broude, E.I. Rashba, E.F. Sheka, *Spectroscopy of Molecular Excitons* (Springer, Berlin, 1985)
6. S. Kirstein, H. Möhwald, Adv. Mater. **7**, 460 (1995)
7. S. Kirstein, H. Mohwald, J. Chem. Phys. **103**, 826 (1995)
8. T. Kobayashi (ed.), *J-Aggregates* (World Scientific, Singapore, 1996)
9. U. Bach, Y. Tachibana, J.-E. Moser, S.A. Haque, J.R. Durant, M. Grätzel, D.R. Klug, J. Am. Chem. Soc. **121**, 7445 (1999)
10. S.A. Haque, Y. Tachibana, R.L. Willis, J.E. Moser, M. Grätzel, D.R. Klug, J.R. Durrant, J. Phys. Chem. B **104**, 538 (2000)
11. W. Gebauer, A. Langner, M. Schneider, M. Sokolowski, E. Umbach, Phys. Rev. B **69**, 155431 (2004)
12. A.A. Vyshkvarko, V.F. Kiselev, V.Z. Paschenko, G.S. Plotnikov, J. Lumin. **47**, 327 (1991)
13. K. Kemnitz, N. Tamai, I. Yamazaki, N. Nakashima, K. Yoshihara, J. Phys. Chem. **90**, 5094 (1986)
14. A. Murayama, Y. Oka, H. Fujisaki, Surf. Sci. **158**, 222 (1985)
15. Y. Liang, A.M. Ponte Goncalves, D.K. Negus, J. Phys. Chem. **87**, 1 (1983)
16. H. Proehl, T. Dienel, R. Nitsche, T. Fritz, Phys. Rev. Lett. **93**, 097403 (2004)
17. G. Bussetti, S. Cirilli, A. Violante, V. Chiostri, C. Goletti, P. Chiaradia, A. Sassella, M. Campione, L. Raimondo, D. Braga, A. Borghesi, J. Vac. Sci. Technol., A **27**, 1029 (2009)
18. M. Schneider, M. Brinkmann, M. Muccini, F. Biscarini, C. Taliani, W. Gebauer, M. Sokolowski, E. Umbach, Chem. Phys. **285**, 345 (2002)
19. U. Heinemeyer, K. Broch, A. Hinderhofer, M. Kytka, R. Scholz, A. Gerlach, F. Schreiber, Phys. Rev. Lett. **104**, 257401 (2010)
20. H. Proehl, R. Nitsche, T. Dienel, K. Leo, T. Fritz, Phys. Rev. B **71**, 165207 (2005)
21. R. Forker, T. Fritz, Phys. Chem. Chem. Phys. **11**, 2142 (2009)
22. M.I. Alonso, M. Garriga, N. Karl, J.O. Osso, F. Schreiber, Org. Electron. **3**, 23 (2002)
23. M.I. Alonso, M. Garriga, J.O. Osso, F. Schreiber, E. Barrena, H. Dosch, J. Chem. Phys. **119**, 6335 (2003)
24. L.D. Sun, M. Hohage, P. Zeppenfeld, S. Berkebile, G. Koller, F.P. Netzer, M.G. Ramsey, Appl. Phys. Lett. **88**, 121913 (2006)
25. L.D. Sun, G. Weidlinger, M. Denk, R. Denk, M. Hohage, P. Zeppenfeld, Phys. Chem. Chem. Phys. **12**, 14706 (2010)

26. W.E. Moerner, T. Basche, Angew. Chem., Int. Ed. **32**, 457 (1993)
27. W. Gebauer, A. Langner, M. Schneider, M. Sokolowski, E. Umbach, Phys. Rev. B **69**, 155431 (2004)
28. T. Dienel, H. Proehl, R. Forker, K. Leo, T. Fritz, J. Phys. Chem. C **112**, 9056 (2008)
29. Z.-C. Dong, X.-L. Guo, A.S. Trifonov, P.S. Dorozhkin, K. Miki, K. Kimura, S. Yokoyama, S. Mashiko, Phys. Rev. Lett. **92**, 086801 (2004)
30. W. Deng, D. Fujita, T. Ohgi, S. Yokoyama, K. Kamikado, S. Mashiko, J. Chem. Phys. **117**, 4995 (2002)
31. E. Ćavar, M.-C. Blüm, M. Pivetta, F. Patthey, M. Chergui, W.-D. Schneider, Phys. Rev. Lett. **95**, 196102 (2005)
32. X.H. Qiu, G.V. Nazin, W. Ho, Science **299**, 542 (2003)
33. C. Chen, P. Chu, C.A. Bobisch, D.L. Mills, W. Ho, Phys. Rev. Lett. **105**, 217402 (2010)
34. F. Rossel, M. Pivetta, W.-D. Schneider, Surf. Sci. Rep. **65**, 129 (2010)
35. R. Nishitani, H.W. Liu, A. Kasuya, H. Miyahira, T. Kawahara, H. Iwasaki, Surf. Sci. **601**, 3601 (2007)
36. W. Gebauer, M. Sokolowski, E. Umbach, Chem. Phys. **227**, 33 (1998)
37. U. Heinemeyer, R. Scholz, L. Gisslén, M.I. Alonso, J.O. Ossó, M. Garriga, A. Hinderhofer, M. Kytka, S. Kowarik, A. Gerlach, F. Schreiber, Phys. Rev. B **78**, 085210 (2008)
38. R. Forker, D. Kasemann, T. Dienel, C. Wagner, R. Franke, K. Müllen, T. Fritz, Adv. Mater. **20**, 1 (2008)
39. D. Schlettwein, H. Tada, S. Mashiko, Thin Solid Films **331**, 117 (1998)
40. S. Tavazzi, A. Borghesi, A. Papagni, P. Spearman, L. Silvestri, A. Yassar, A. Camposeo, M. Polo, D. Pisignano, Phys. Rev. B **75**, 245416 (2007)
41. E. Engel, K. Schmidt, D. Beljonne, J.L. Bredas, J. Assa, H. Frob, K. Leo, M. Hoffmann, Phys. Rev. B **73**, 245216 (2006)
42. T. Petrenko, O. Krylova, F. Neese, M. Sokolowski, New J. Phys. **11**, 015001 (2009)
43. D. Käfer, G. Witte, Phys. Chem. Chem. Phys. **7**, 2850 (2005)
44. O.D. Jurchescu, A. Meetsma, T.T.M. Palstra, Acta Crystallogr. B **62**, 330 (2006)
45. E. Venuti, R.G. Della Valle, L. Farina, A. Brillante, M. Masino, A. Girlando, Phys. Rev. B **70**, 104106 (2004)
46. O. Worz, G. Scheibe, Z. Naturforsch. B **24**, 381 (1969)
47. A. Kraft, R. Temirov, S.K.M. Henze, S. Soubatch, M. Rohlfing, F.S. Tautz, Phys. Rev. B **74**, 041402(R) (2006)
48. E. Umbach, M. Sokolowski, R. Fink, Appl. Phys. Lett. A **63**, 565 (1996)
49. G. Witte, C. Wöll, J. Mater. Res. **19**, 1889 (2004)
50. D.E. Hooks, T. Fritz, M.D. Ward, Adv. Mater. **13**, 227 (2001)
51. S.C.B. Mannsfeld, K. Leo, T. Fritz, Phys. Rev. Lett. **94**, 056104 (2005)
52. D. Schlettwein, A. Back, B. Schilling, T. Fritz, N.R. Armstrong, Chem. Mater. **10**, 601 (1998)
53. T. Dienel, C. Loppacher, S.C.B. Mannsfeld, R. Forker, T. Fritz, Adv. Mater. **20**, 959 (2008)
54. A. Langner, Y. Su, M. Sokolowski, Phys. Rev. B **74**, 2633 (2006)
55. S. Degen, A. Krupski, M. Kralj, A. Langner, C. Becker, M. Sokolowski, K. Wandelt, Surf. Sci. Lett. **576**, L57 (2005)
56. J. Kramer, C. Tegenkamp, H. Pfnür, J. Phys., Condens. Matter **38**, 6473 (2003)
57. M. Pivetta, F. Patthey, M. Stengel, A. Baldereschi, W.-D. Schneider, Phys. Rev. B **72**, 115404 (2005)
58. E. Le Moal, M. Müller, O. Bauer, M. Sokolowski, Surf. Sci. **603**, 2434 (2009)
59. M. Müller, J. Ikonomov, M. Sokolowski, Surf. Sci. **605**, 1090 (2011)
60. M. Bäumer, H.J. Freund, Prog. Surf. Sci. **61**, 127 (1999)
61. J. Repp, G. Meyer, Phys. Rev. Lett. **94**, 026803 (2005)
62. S.A. Burke, J.M. Topple, P. Grütter, J. Phys., Condens. Matter **21**, 423101 (2009)
63. A. Langner, A. Hauschild, S. Fahrenholz, M. Sokolowski, Surf. Sci. **574**, 153 (2005)
64. M. Voigt, A. Langner, P. Schouwink, J. Lupton, R. Mahrt, M. Sokolowski, J. Chem. Phys. **127**, 114705 (2007)
65. S.-H. Lim, T.G. Bjorklund, F.C. Spano, C.J. Bardeen, Phys. Rev. Lett. **92**, 107402 (2004)
66. F. Spano, Annu. Rev. Phys. Chem. **57**, 217 (2006)
67. S. Soubatch, C. Weiss, R. Temirov, F.S. Tautz, Phys. Rev. Lett. **102**, 177405 (2009)
68. V. Czikkely, H.D. Försterling, H. Kuhn, Chem. Phys. Lett. **6**, 11 (1970)
69. F. Meinardi, M. Cerminara, A. Sassella, R. Bonifacio, R. Tubino, Phys. Rev. Lett. **91**, 247401 (2003)
70. P.B. Walczak, A. Eisfeld, J.S. Briggs, J. Chem. Phys. **128**, 044505 (2008)
71. E.W. Knapp, Chem. Phys. **85**, 73 (1984)
72. F.C. Spano, J.R. Kuklinski, S. Mukamel, Phys. Rev. Lett. **65**, 211 (1990)
73. F.C. Spano, J. Chem. Phys. **120**, 7643 (2004)
74. M. Kytka, L. Gisslen, A. Gerlach, U. Heinemeyer, J. Kováč, R. Scholz, F. Schreiber, J. Phys. Chem. **130**, 214507 (2009)
75. H. Najafov, I. Biaggio, V. Podzorov, M.F. Calhoun, M.E. Gershenson, Phys. Rev. Lett. **96**, 056604 (2006)
76. R.R. Chance, A. Prock, R. Silbey, Adv. Chem. Phys. **37**, 1 (1978)
77. S. Soubatch, R. Temirov, M. Weinhold, F.S. Tautz, Surf. Sci. **600**, 4679 (2006)
78. E. Le Moal, M. Müller, O. Bauer, M. Sokolowski, Phys. Rev. B **82**, 045301 (2010)
79. S.A. Burke, W. Ji, J.M. Mativetsky, J.M. Topple, S. Fostner, H.-J. Gao, H. Guo, P. Grutter, Phys. Rev. Lett. **100**, 186104 (2008)
80. M. Müller, E. Le Moal, R. Scholz, M. Sokolowski, Phys. Rev. B **83**, 241203(R) (2011)
81. K. Glöckler, C. Seidel, A. Soukopp, M. Sokolowski, E. Umbach, M. Böhringer, R. Berndt, W.-D. Schneider, Surf. Sci. **405**, 1 (1998)
82. A. Kraft, R. Temirov, S.K.M. Henze, S. Soubatch, M. Rohlfing, F.S. Tautz, Phys. Rev. B **74**, 041402 (2006)
83. J. Ikonomov, O. Bauer, M. Sokolowski, Surf. Sci. **602**, 2061 (2008)
84. M. Müller, Ph.D. thesis, University of Bonn, in preparation
85. R. Scholz, A.Y. Kobitski, T.U. Kampen, M. Schreiber, D.R.T. Zahn, G. Jungnickel, M. Elstner, M. Sternberg, T. Frauenheim, Phys. Rev. B **61**, 13659 (2000)
86. I. Vragovic, R. Scholz, Phys. Rev. B **68**, 155202 (2003)
87. M. Wewer, F. Stienkemeier, J. Chem. Phys. **120**, 1239 (2004)
88. M. Dvorak, F. Stienkemeier, Unpublished results (2009)
89. A. Langner, Ph.D. thesis, Universität Bonn, 2005
90. O. Krylova, Ph.D. thesis, University of Bonn, in preparation
91. M. Müller, Diploma thesis, University of Bonn, 2007